

SEMIQUANTITATIVE ELECTRON MICROPROBE DETERMINATION OF $\text{Fe}^{2+}/\text{Fe}^{3+}$ AND $\text{Mn}^{2+}/\text{Mn}^{3+}$ IN OXIDES AND SILICATES AND ITS APPLICATION TO PETROLOGIC PROBLEMS¹

ARDEN L. ALBEE AND ARTHUR A. CHODOS, *Division of Geological Sciences, California Institute of Technology, Pasadena, California 91109*

ABSTRACT

The relative intensities of FeL_α and L_β X-ray emission peaks differ significantly with valence state and bond association, even though the wavelength shift is very small. $\text{L}_\beta/\text{L}_\alpha$ increases systematically with increase in $\text{Fe}^{2+}/\text{Fe}^{3+}$ or $\text{Mn}^{2+}/\text{Mn}^{3+}$ in their respective oxides, in the hematite-ilmenite series, in the magnetite-ulvospinel series, and in anhydrous silicates. $\text{Fe L}_\beta/\text{L}_\alpha$ ratios are much higher for Fe-O-Si and Fe-O-Ti bond associations than for Fe-O-Fe. $\text{L}_\beta/\text{L}_\alpha$ ratios clearly distinguish ferric-rich alkali amphiboles from ferrous-rich calciferous amphiboles. No significant variation was found for the individual mineral types—chloritoid, staurolite, and cordierite, but a variation does occur in chlorite. Ferric-rich muscovite is not distinguishable from ferrous-rich biotite.

INTRODUCTION

Even semiquantitative determination of the oxidation state of Fe and Mn by the electron microprobe would have important applications to petrologic and mineralogic problems. Andersen (1966) pointed out that the relative intensities of Fe L_α and L_β X-ray emission peaks differ significantly with valence state in metallic Fe, FeS_2 , Fe_2O_3 , and Fe_3O_4 . We extended his work to other Fe and Mn oxides and synthetic silicates (Albee, Chodos, and Smith, 1967) and utilized it in a petrologic problem (Smith and Albee, 1967). This note summarizes our results to date and our evaluation of the utility of the technique.

The commercial electron microprobe can provide information on crystal structure and bonds from the X-ray emission peaks that could previously only be obtained on specialized research instruments (Dodd and Glen, 1968; White and Gibbs, 1967, 1969). The wavelength of the emission peak is related to the difference in energy between the energy states of the atom, and the relative peak intensities are related to the transition probabilities between energy states; hence the detailed peak shape is a function of both variations in energy difference and transition probabilities (see the review paper by Parratt, 1959; see also Fabian, 1968). From a mineralogic point of view, the position, shape, and relative intensity of the peak may depend upon the coordination number, the identity of the nearest neighbors, the bond length, the bond angle, and the bond type, as well as the valence. In addition the measured spectra may include the effects of absorption and fluorescence within the sample.

¹ Contribution Number 1662.

It is difficult to completely separate the effect of valence from other effects. There are probably no silicates in which there is a complete variation from divalent to trivalent Fe or Mn without a systematic variation in other structural parameters. Divalent and trivalent Fe and Mn differ in ionic radii as well as in charge and commonly play very different roles in rock-forming silicates and oxides. As illustrated in Figure 1, many silicates have an essentially divalent, six- or eight-fold coordinated position which may be occupied by Fe^{2+} , Mn^{2+} , Mg, Ca, etc., whereas others have an essentially trivalent six-fold coordinated position which may be occupied by Al, Fe^{3+} , Mn^{3+} , etc. A few minerals such as garnet contain both types of positions. In addition trivalent Fe can occur in primarily divalent positions by several types of coupled substitutions as

| Role of Fe in Silicates | |
|---|--|
| Fe^{+2} (0.83 Å; VI, rarely VIII) | Fe^{+3} (0.67 Å; VI, rarely IV) |
| Role: $\text{Fm} \equiv \text{Fe}^{+2}$, Mg, Mn, Ca, Ni, ... i.e.: hypersthene $\text{Fm}_2\text{Si}_2\text{O}_6$ i.e.: garnet $\text{Fm}_3(\text{Al}, \text{Fe}^{+3})_2(\text{SiO}_4)_3$ | Role: $\text{Fe}^{+3} \leftrightarrow \text{Al}$ i.e.: epidote $\text{Ca}_2(\text{Al}, \text{Fe}^{+3})_3(\text{SiO}_4)(\text{Si}_2\text{O}_7)(\text{OH})$ |
| Role: $[\text{Fe}^{+3} \text{ for } \text{Fm}^{+2}]^{\text{VI}} \leftrightarrow [\text{Na}^{+1} \text{ for } \text{Fm}^{+2}]^{\text{VI, VIII}}$ Role: $[\text{Fe}^{+3} \text{ for } \text{Fm}]^{\text{VI}} \leftrightarrow [\text{Al}^{\text{IV}} \text{ for } \text{Si}]^{\text{IV}}$ | |
| i.e.: acmite-augite $(\text{Ca}_{4-x}\text{Na}_x)(\text{Fm}_{4-x}\text{Fe}_x^{+3})(\text{Si}_2\text{O}_6)$ i.e.: augite $(\text{Ca}_{4-x}\text{Na}_x)(\text{Fm}_{4-x-y})(\text{Al}, \text{Fe}^{+3})_{x+y}(\text{Si}_{2-y}\text{Al}_y\text{O}_6)$ | i.e.: enstatite $(\text{Mg}_{2-y}\text{Fe}_y^{+3})(\text{Al}_y\text{Si}_{2-y}\text{O}_6)$ |
| Role: $[\text{Fe}^{+2} \leftrightarrow \text{Fe}^{+3}]$ with loss of H^+ | |
| Biotite: $\text{K}^{\text{XIII}} [(\text{Fm}_{3-x-y})(\text{Al}, \text{Fe}^{+3})_x(\text{Fe}_y^{+3})]^{\text{VI}} [\text{Al}_{1+x}\text{Si}_{3-x}]^{\text{IV}} \text{O}_{12}\text{H}_{2-y}$ Hornblende: $\text{Na}_{x+y}^{\text{XII}} \text{Ca}_z^{\text{XIII}} [\text{Fm}_{5-x-z-w}(\text{Al}, \text{Fe}^{+3})_{x+z}\text{Fe}_w^{+3}]^{\text{VI}} [\text{Al}_y\text{Si}_{8-y-z}]^{\text{IV}} \text{O}_{24}\text{H}_{2-w}$ | |

Fig. 1. Different roles of divalent and trivalent iron in silicates.

illustrated on Figure 1. In pyroxenes, for example, Fe^{3+} occurs in the Fm position by coupled substitution of a univalent ion (Na) for a divalent ion or of a trivalent ion (Al) for a quadrivalent ion (Si). In many hydrous minerals the substitution of Fe^{3+} for Fe^{2+} can be balanced by a proton deficiency. The oxidation of Fe^{2+} to Fe^{3+} can occur upon heating in air, and it has been demonstrated for some minerals that the reaction can be reversed in a hydrogen atmosphere.

In order to distinguish the valence effect from other structural effect, L_β/L_α intensity ratios were measured for Fe and Mn oxides and a wide variety of Fe- and Mn-bearing silicates, including many synthetic minerals as well as analyzed natural samples. Figure 2 shows the L_α - L_β peaks for Fe and Mn metals and their various oxides. The samples are synthetic pure samples with the exception of hematite and magnetite, which are well-analyzed probe standards. The figure was prepared by projecting profiles to a common height; hence the wavelength scale is variable and

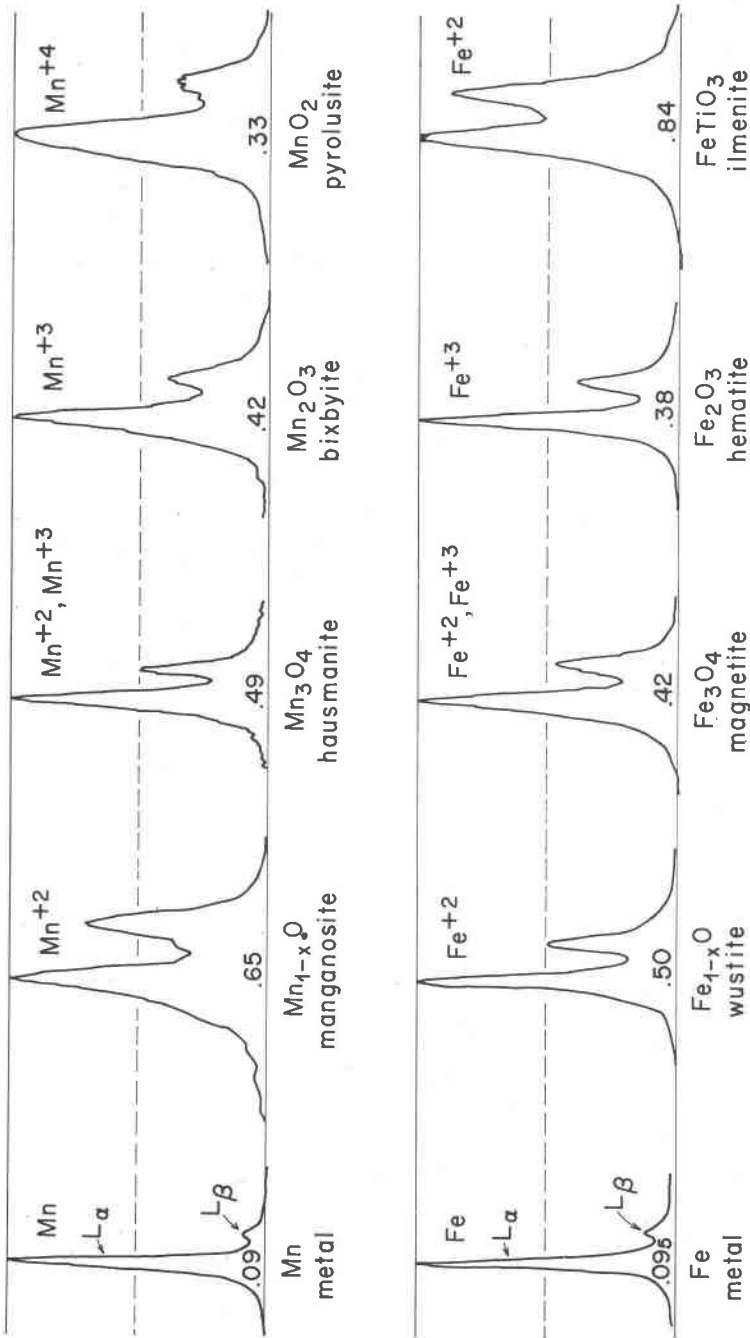


Fig. 2. Microprobe wavelength scans for the $L\alpha$ and $L\beta$ emission peaks of Fe and Mn in oxides and metal. All $L\alpha$ peaks are projected to a common height above background and the horizontal wavelength scale varies from profile to profile.

peak shapes cannot be compared on the figure. The relative peak heights for the oxides are very different from those for the metals, and in addition L_{β}/L_{α} decreases systematically with increasing valence. Magnetite and hausmanite, which contain both divalent and trivalent Fe or Mn, have intermediate values. Ilmenite has also been included to illustrate the marked difference between the Fe L_{β}/L_{α} ratio for the Fe—O—Ti bond association and the Fe—O—Fe bond association. The L_{β}/L_{α} values shown on the figure were obtained by step-counting, not from the individual profile shown.

Figure 3 shows spectra for some end-member silicates. Both divalent and trivalent Fe (or Mn) are in six-fold coordination in their respective end-members and all, except piemontite, are anhydrous. The L_{β}/L_{α} ratio is quite different from that in the oxides, but similar to that in ilmenite. Like the oxides the Fe and Mn L_{β}/L_{α} is smaller in the trivalent end-members than in the divalent end-members.

EXPERIMENTAL PROCEDURE

The L_{β}/L_{α} values were determined at 15 kV on an Applied Research Laboratory model EMX microprobe, using a KAP crystal and pulse-height selection. The observed L_{β}/L_{α} ratio varies markedly with accelerating voltage, and the relationship to valence may also change (Fischer, 1965, Fig. 7). Hence, these results are only applicable at 15 kV. The specimen current and spot size were adjusted to give reasonable intensity without specimen damage.

Intensity ratios can be obtained either by measuring peak heights on a wavelength profile from a chart recorder or by step-counting across the peaks. Most of the samples shown in Figures 4 and 5 were analyzed both by:

- 1) measuring peak heights on profiles run from high-wavelength to low-wavelength and reverse, and;
- 2) running a chart profile to locate the peaks and then step-counting across the crest of the peaks and in background locations on either side.

In general, three to six points on a number of grains were averaged for the first method, and at least three points were averaged for the second method. In most cases the averages are similar, but the variation is substantially less by the second method. Intensity loss due to carbon contamination build up was controlled by a large spot size and by not step-counting across the entire L_{α} - L_{β} profile, but the use of a cold-trap would be beneficial.

In this reconnaissance study, enough repeat measurements were made to ensure that the values shown in Figures 4 and 5 are within five percent of their correct value. The values for most of the hydrous minerals shown in Figures 6 and 7 were obtained by the chart method using fewer profiles and the errors may be as much as ten percent. For these samples, inhomogeneity, impurities, and spectrometer gearing are possible sources of error. In addition, because of the low intensity of L lines and lower Fe concentration in some of these samples, some contribution may occur from other elements despite the use of pulse height selection.

RESULTS AND DISCUSSION

Measured L_{β}/L_{α} values for oxides and simple, predominantly anhydrous, silicates of iron and manganese are shown on Figure 4. Most of

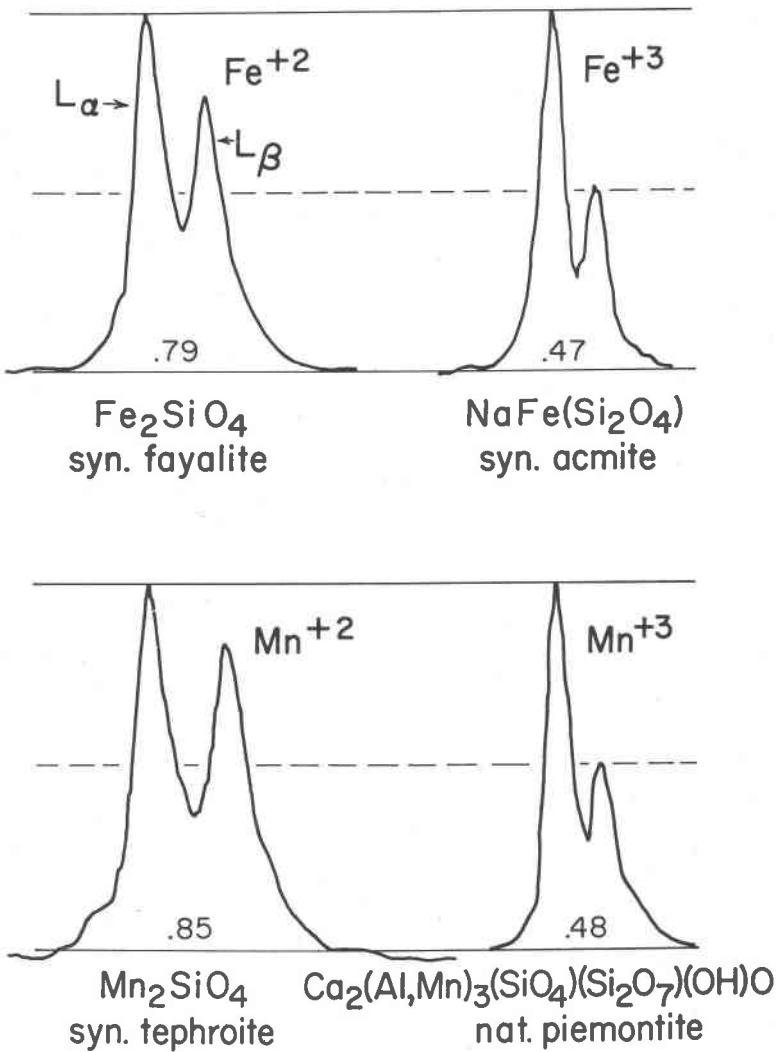


Fig. 3. Microprobe wavelength scans for the L_{α} and L_{β} emission peaks of Fe and Mn in simple silicates. All L_{α} peaks are projected to a common height above background and the horizontal wavelength scale varies from profile to profile.

the samples used are synthetic; they have not been analyzed and stoichiometry has been assumed. As shown L_{β}/L_{α} increases systematically with increase in Fe^{2+}/Fe^{3+} or Mn^{2+}/Mn^{3+} in their respective oxides. Two values are shown for hausmanite. The higher value was measured in July, 1967; the lower value was obtained in several measurements in July,

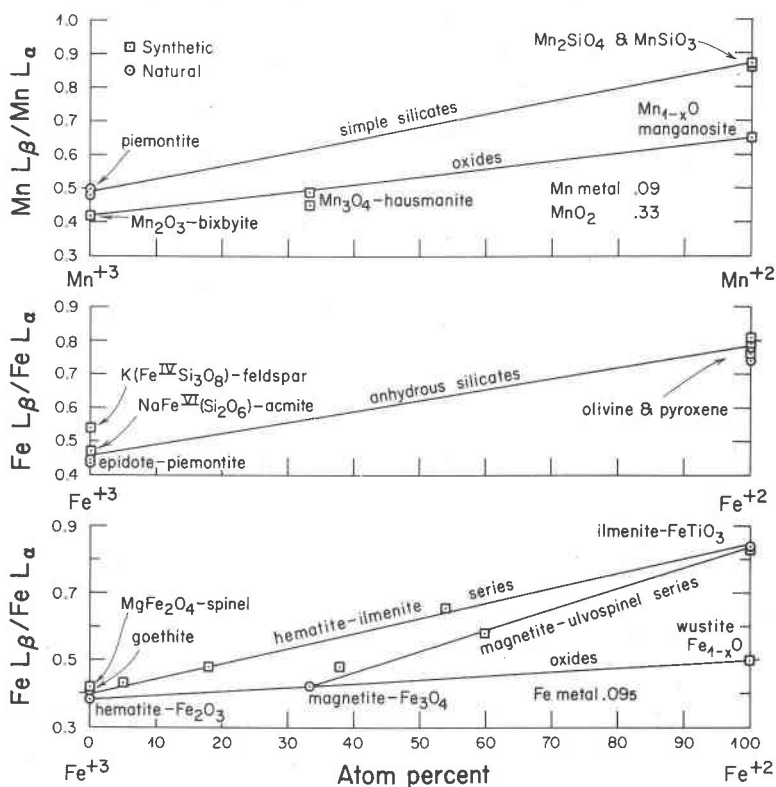


Fig. 4. L_{β}/L_{α} ratios for oxides and simple silicates of Fe and Mn.

1969. It seems quite possible that the higher value is the correct value and that the surface of the small grains in the grain mount has oxidized to bixbyite in the intervening time. However, the grains are anisotropic in reflected light. A systematic variation also occurs in the hematite-ilmenite series and the magnetite series as indicated by data on synthetic phases of intermediate composition. The $Fe L_{\beta}/L_{\alpha}$ ratios are markedly higher for the $Fe-O-Ti$ bond association than for the $Fe-O-Fe$ bond association. The variation shown here is large enough to be useful in the analysis and identification of opaque minerals in petrologic and paleomagnetic studies. It might also prove very useful in the study of sea-floor manganese nodules.

The L_{β}/L_{α} values are also much higher for the silicates than for oxides and are much higher for the $Fe^{2+}-O-Si$ (and $Mn^{2+}-O-Si$) bond association than for the $Fe^{3+}-O-Si$ (or $Mn^{3+}-O-Si$) bond association. However, the associated L_{α} wavelength shift is only about 0.035 \AA (see

also Fischer, 1965). Most of the sample points shown are synthetic minerals with Fe or Mn six-fold coordination with oxygen. A synthetic Fe microcline, which has Fe^{3+} in four-fold coordination, has a somewhat higher L_{β}/L_{α} value than does synthetic acmite, which has Fe^{3+} in six-fold coordination.

Relatively few anhydrous silicates have a wide continuous variation in Fe^{2+}/Fe^{3+} , but the method should be useful for garnets and pyroxenes and for helping to characterize unknown anhydrous minerals. Since we do not have synthetic samples of these minerals with intermediate values of Fe^{2+}/Fe^{3+} , we have made a reconnaissance study of some chemically

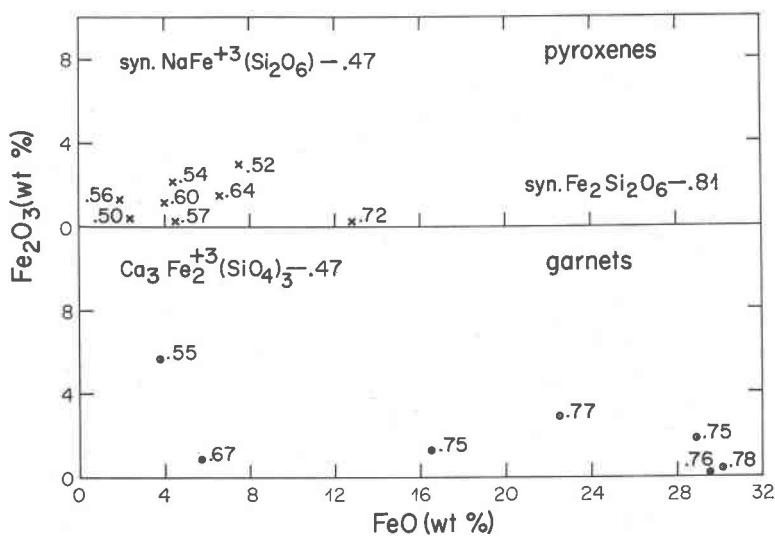


Fig. 5. L_{β}/L_{α} ratios for chemically-analyzed garnets and pyroxenes.

analyzed minerals. Figure 5 shows L_{β}/L_{α} values for a number of chemically-analyzed garnets and pyroxenes with a range in FeO/Fe_2O_3 . The results indicate that predominantly ferrous and predominantly ferric garnet and pyroxene can be distinguished. However, it is clear that better standards and better L_{β}/L_{α} measurements are necessary to really test the usefulness of the method.

Hydrous minerals have a wide range of Fe^{2+}/Fe^{3+} , and a microprobe technique capable of measuring this ratio in these minerals would be most valuable to the petrologist. Figure 6 shows L_{β}/L_{α} ratios for a number of chemically analyzed amphiboles. In general, the alkali amphiboles with their higher ferric iron content have quite different L_{β}/L_{α} ratios than do the calciferous amphiboles and the one example of cumming-

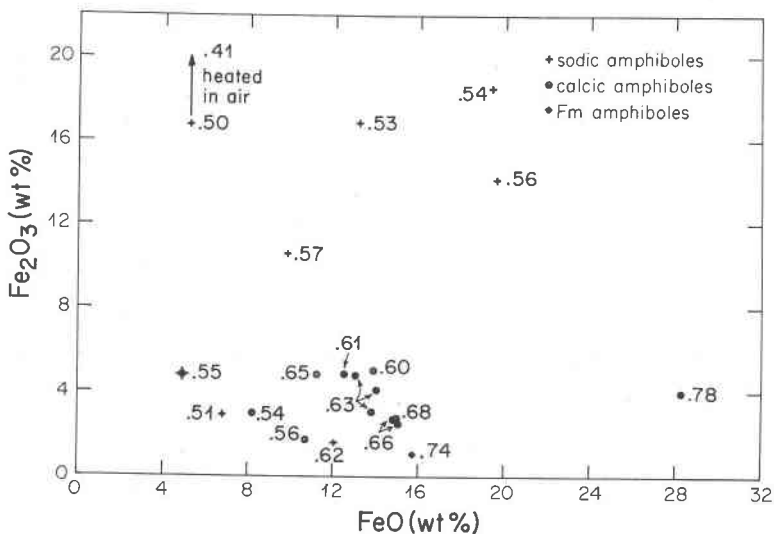


Fig. 6. L_{β}/L_{α} ratios for chemically-analyzed amphiboles.

tonite. One alkali amphibole was analyzed both before and after oxidation by heat treatment and the L_{β}/L_{α} ratio changed in the predicted direction. As with the garnets and pyroxenes, however, it would be necessary to have standards with better known $\text{FeO}/\text{Fe}_2\text{O}_3$ contents and to determine the L_{β}/L_{α} ratio more accurately in order to test the usefulness of the method within groups.

Figure 7 shows data for a number of other hydrous minerals. The ratios were measured by the profile method and are not accurate enough to demonstrate a real variation for the individual mineral types—cordierite, chloritoid, and staurolite. The staurolite samples, taken as a group, show a lower L_{β}/L_{α} than do the chloritoid samples, taken as a group, and this is consistent with the chemical data in suggesting a higher ferric iron content. Mössbauer work on staurolite has not indicated the presence of Fe^{3+} (Smith, 1969, p. 1145), and the Fe^{3+} has been attributed to errors in the chemical determination. Since the Mössbauer work was apparently done on gem-quality samples, it is possible that more typical staurolite samples do contain Fe^{3+} . Four-fold coordinated Fe^{3+} has a higher L_{β}/L_{α} than does six-fold coordinated Fe^{3+} , so it seems rather unlikely that the effect of the four-fold coordinated Fe^{2+} in staurolite (Smith, 1969) accounts for the difference between staurolite and chloritoid.

The chlorite samples analyzed show a rather good correlation between the chemically-determined $\text{FeO}/\text{Fe}_2\text{O}_3$ and the L_{β}/L_{α} ratio. The results suggest that useful results might be obtainable on this mineral.

The upper part of Figure 7 shows L_{β}/L_{α} values for analyzed muscovite

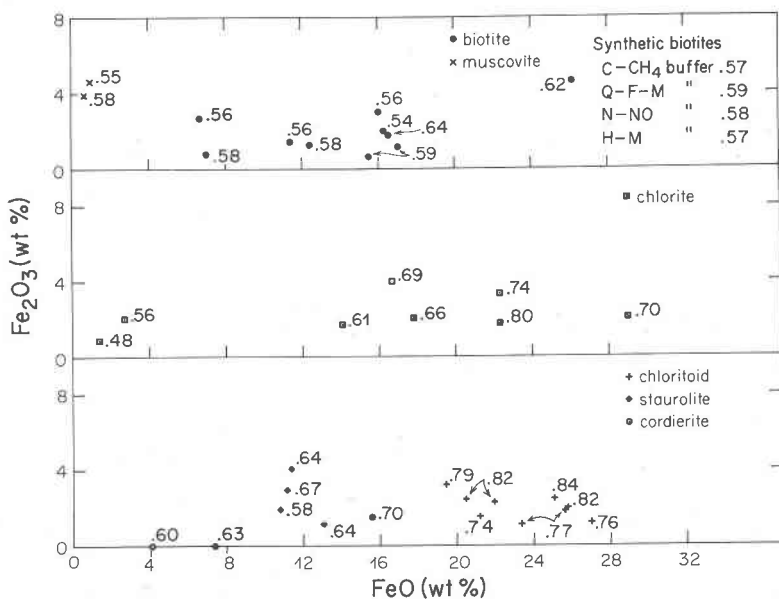


Fig. 7. L_{β}/L_{α} ratios for chemically-analyzed hydrous silicates.

and biotite samples. The values for muscovite, which should be predominantly ferric, overlap those for biotite, which should be predominantly ferrous. This overlap of values measured on profiles has been confirmed by step-count measurements on several samples. In addition, the values shown on Figure 8 for biotites synthesized at very different oxygen activities were obtained by step-counting and do not show significant differences in L_{β}/L_{α} . The valence effect in hydrous minerals might be obscured by the coordination of Fe with OH, rather than O, or by oxidation of iron by the electron beam during the analysis. However, the apparent partial success of the method on amphiboles and chlorite make these suggestions seem unlikely. The fifth order of potassium K_{β} would coincide with the Fe L_{β} and, despite the use of pulse height selection, might be significant in muscovite with a low iron content. However, this should increase the L_{β}/L_{α} in muscovite, which is the reverse of the observed relationship. Jack Leitner, Applied Research Laboratories, kindly analyzed a muscovite and a biotite and obtained similar results, using an RAP crystal rather than a KAP crystal.

The results of this survey of a number of natural minerals are encouraging—except for the micas. However, for useful results, the ratios must be measured more accurately by longer step-counting and by controlling carbon contamination during the counting.

There seems to be no adequate theory which would have predicted the

results which were obtained. L_{β_1} results from the $L_{II}-M_{IV}$ transition and $L_{\alpha_{1,2}}$ results from the $L_{III}-M_{V,IV}$ transition. Their relative intensity should to a first approximation be related to the relative number of electrons in the L_{II} and L_{III} subshells, which would give a L_{β}/L_{α} ratio of 0.50. The lower than predicted L_{β}/L_{α} ratio for metals (about 0.09 for Fe and Mn) has been explained as due to an Auger transition (Fischer, 1965, p. 2053), with part of the intensity "robbed" from the L_{β} peak reappearing as part of the L_{α} peak (Parratt, 1959, p. 635). However, the L_{III} absorption edges for iron and manganese lie between their L_{α} and L_{β} peaks and may produce a strong effect on the relative intensities. Andersen and Wittry (1968, p. 538) have shown that the absorption-corrected L_{β}/L_{α} intensity for metallic iron is about 0.30, rather than the observed 0.09, and that the absorption-corrected intensity ratio appears to be essentially independent of accelerating potential. In general, the absorption correction is probably large enough that accurate absorption corrections will have to be applied to the measured relative intensities before an adequate theory can be formulated.

Snetsinger (1969) has suggested that since there are more electrons in the outer M subshell if Fe is divalent rather than trivalent, the intensity of $L_{\alpha_{1,2}}$ would be greater for Fe^{2+} than for Fe^{3+} ; i.e., L_{β}/L_{α} would increase for increasing oxidation state. This is the relationship shown between Fe and Fe^{2+} , but the reverse relationship occurs for Fe^{2+} and Fe^{3+} .

ACKNOWLEDGMENTS

We are indebted to numerous individuals who have provided synthetic or chemically-analyzed standards; in particular, D. H. Lindsley for synthetic Fe-Ti oxides, J. S. Huebner for synthetic Mn oxides and silicates, M. Rutherford for synthetic biotites, D. R. Wones for synthetic Fe-microcline, and W. G. Ernst and A. E. J. Engel for analyzed amphiboles. Douglas Smith participated in early phases of the investigations, and Lily Ray made many of the analyses. The investigation was supported by National Science Foundation grant G-3570.

REFERENCES

- ALBEE, A. L., A. A. CHODOS, AND DOUGLAS SMITH, (1967) Semiquantitative electron microprobe determinations of Fe^{2+}/Fe^{3+} and Mn^{2+}/Mn^{3+} in silicates and their application to petrologic problems (abstr). *Geol. Soc. Amer. Spec. Pap.* **115**, 2-3.
- ANDERSEN, C. A. (1966) The quality of X-ray microanalysis in the ultrasoft X-ray region. [abstr.] *First National Conference on Electron Probe Microanalysis, College Park, Maryland*.
- (1967) The quality of X-ray microanalysis in the ultrasoft X-ray region. *Brit. J. Appl. Phys.* **18**, 1033-1043.
- and D. B. WITTRY, (1968) An evaluation of absorption correction functions for electron probe microanalysis. *Brit. J. Appl. Phys., Ser. 2*, **1**, 529-540.
- DODD, C. G. AND G. L. GLEN, (1968) Chemical bonding studies of silicates and oxides by X-ray K-emission spectroscopy. *J. Appl. Phys.* **39**, 5377-5384.

- FABIAN, D. J., ed. (1968) *Soft X-ray Band Spectra and the Electronic Structure of Metals and Materials*. Academic Press, New York, 382 p.
- FISCHER, D. W. (1965) Changes in the soft X-ray L-emission spectra with oxidation of the first series transition metals. *J. Appl. Phys.* **36**, 2048-2053.
- PARRATT, L. G. (1959) Electronic band structure of solids by X-ray spectroscopy. *Rev. Mod. Phys.* **31**, 616-645.
- SMITH, DOUGLAS AND A. L. ALBEE, (1967) Petrology of a piemontite-bearing gneiss, San Geronio Pass, California: *Contrib. Mineral. Petrology* **16**, 189-203.
- SMITH, J. V. (1968) The crystal structure of staurolite. *Amer. Mineral.*, **53**, 1139-1155.
- SNETSINGER, K. G. (1969) Manganoan ilmenite from a Sierran adamellite. *Amer. Mineral.*, **54**, 431-436.
- WHITE, E. W. AND G. V. GIBBS, (1967) Structural and chemical effects of the Si K_{β} X-ray line for silicates. *Amer. Mineral.* **52**, 985-993.
- AND ——— (1969) Structural and chemical effects on the Al K_{β} X-ray emission band among aluminum-containing silicates and aluminum oxides. *Amer. Mineral.* **54**, 931-936.

Manuscript received, September 18, 1969; accepted for publication October 29, 1969.